Sl. No.	IIT Ropar List of Recent Publications with Abstract Coverage: November, 2020
1.	A Modular Converter Topology with Fast Discharging and Regenerative Capability for any n-Phase SRM Drive AK Rana, AVR Teja - The 46th Annual Conference of the IEEE Industrial Electronics Society, 2020 **Abstract:** This paper presents a novel converter topology having less switches per phase and a common fast discharging circuit suitable for Switched Reluctance Motor (SRM) drives. The topology makes use of fly back circuit principle for fast discharge of winding current back to the source. The proposed topology can be modularized for any n-phase SRM drive keeping the same discharging circuit. The converter is analyzed and is implemented on a 4 phase 8/6 SRM drive using PSPICE and MATLAB/Simulink and the results are reported.
2.	A Novel Direct Torque Control for 4-Phase Switched Reluctance Motor Considering the Actual Rotor Pole Arc with High Torque/Ampere Ratio V Shah, S Payami - The 46th Annual Conference of the IEEE Industrial Electronics Society, 2020 **Abstract:** Most of the direct and indirect torque control schemes proposed for switched reluctance motors (SRMs) consider equal rotor and stator pole arc. Leading to a linear non-saturating inductance profile. However, actually, in SRM, the rotor pole arc is kept higher than the stator pole arc. Leading to a non-linear saturating inductance profile. And not considering this in control leads to underutilization of the maximum torque producing capacity during the constant torque region. In the proposed novel direct torque control (DTC) scheme, firstly, the rotor pole arc and saturation effect are incorporated by considering it in the sector formation for every electrical cycle. Second, the flux control loop is removed, and sectors are classified based on the actual inductance profile, which is rotor position-dependent. Also, the voltage vector selection rule is modified for torque control. And the proposed voltage vector concerning the sector, allows multiple phases to conduct simultaneously. Wherein each phase conducts according to its actual inductance profile. This also ensures complete energization of incoming phase current while the outgoing phase is maintained at a constant current level. Leading to a reduction in torque ripples during commutation. The proposed DTC scheme incorporating the rotor pole arc and saturation effect improves the operating range for effectively reducing the torque ripples and facilitates a higher torque/ampere ratio.
3.	A Review on alloy design, biological response, and strengthening of β-Titanium Alloys as biomaterials SS Sidhu, H Singh, MAH Gepreel - Materials Science and Engineering: C, 2020 **Abstract:** From the past few years, developments of β-Ti alloys have been the subject of active research in the medical domain. The current paper highlights significant findings in the area of β-Ti alloy design, biological responses, strengthening mechanisms, and developing low-cost implants with a high degree of biocompatibility. It is evident that an astonishing demand for developing the low modulus-high strength implants can be fulfilled by synchronizing β stabilizer content and incorporating tailored thermo-mechanical techniques. Furthermore, the biological response of the implants is as important as the physical properties that regulate healing response;

	hence, the optimum selection of alloying elements plays a curial role for clinical success. The paper also presents the evolution of patents in this field from the year 2010 to 2020 showing the relevant innovations that may benefit a wide range of researchers. **Graphical Abstract:** 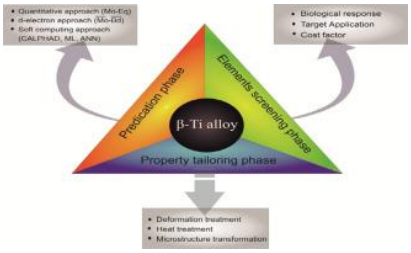
4.	Activity-selection Behavior and Optimal User-distribution in Q&A Websites A Chhabra, SRS Iyengar, JS Saini, V Malik - International Conference on Computational Collective Intelligence: Part of the Lecture Notes in Computer Science book series, 2020 **Abstract:** Based on various factors such as experience, interest, and motivation, users in any system choose to perform certain activities more than the others. In this study, we investigate a similar behavior and its dynamics in the websites of StackExchange. We find that most of the users in these websites tend to contribute predominantly to one of the activities available on these websites. Such a behavior yields a high-level distribution of users across the activities, referred to as User-distribution. We find that this distribution varies for different websites of StackExchange. We also observe that the users contributing to different activities trigger each other to provide more contribution. Using these insights, we build a model that explains the effect of change in user-distribution on the amount of knowledge produced on these websites. The model shows that one can formulate an optimal ecosystem by motivating the right kind of users, which leads to the maximum fostering of knowledge on these websites.
5.	All-in-One UHF RFID Tag Antenna for Retail Garments Using Nonuniform Meandered Lines M Kumar, A Sharma, IJG Zuazola - Progress In Electromagnetics Research, 2020 **Abstract:** An all-in-one UHF RFID tag antenna using nonuniform meandered lines for retail garments in the textile industry is presented. The all-in-one antenna offers relatively low cost, wide band, compactness, and good conjugate matching in the presence of its robust housing with good dipolelike read range. Results show an antenna with a wide bandwidth of 900 MHz and a long read range of 10.2 m making the UHF RFID tag antenna using nonuniform meandered lines a potential candidate for retail garments in the textile industry. Simulations are corroborated by measurements and are in fair agreement.
6.	An End-to-End Edge Aggregation Network for Moving Object Segmentation PW Patil, KM Biradar, A Dudhane, S Murala - Proceedings of the IEEE/CVF Conference on Computer Vision and Pattern Recognition (CVPR), 2020 **Abstract:** Moving object segmentation in videos (MOS) is a highly demanding task for security-based applications like automated outdoor video surveillance. Most of the existing techniques proposed for MOS are highly depend on fine-tuning a model on the first frame(s) of test sequence or complicated training procedure, which leads to limited practical serviceability of the algorithm. In this paper, the inherent correlation learning-based edge extraction mechanism

	(EEM) and dense residual block (DRB) are proposed for the discriminative foreground representation. The multi-scale EEM module provides the efficient foreground edge related information (with the help of encoder) to the decoder through skip connection at subsequent scale. Further, the response of the optical flow encoder stream and the last EEM module are embedded in the bridge network. The bridge network comprises of multi-scale residual blocks with dense connections to learn the effective and efficient foreground relevant features. Finally, to generate accurate and consistent foreground object maps, a decoder block is proposed with skip connections from respective multi-scale EEM module feature maps and the subsequent down-sampled response of previous frame output. Specifically, the proposed network does not require any pre-trained models or fine-tuning of the parameters with the initial frame(s) of the test video. The performance of the proposed network is evaluated with different configurations like disjoint, cross-data, and global training-testing techniques. The ablation study is conducted to analyse each model of the proposed network. To demonstrate the effectiveness of the proposed framework, a comprehensive analysis on four benchmark video datasets is conducted. Experimental results show that the proposed approach outperforms the state-of-the-art methods for MOS.
7.	Analytical Approach for Common Mode EMI Noise Analysis in Dual Active Bridge Converter B Dwiza, J Kalaiselvi - The 46th Annual Conference of the IEEE Industrial Electronics Society, 2020 **Abstract:** The increased demand for high power density converters resulted in increased EMI. This is addressed by considering all the converter parasitics along the noise propagation path. In this paper, the analytical approach for common mode (CM) noise analysis of dual active bridge (DAB) converter is presented. The dv/dt of CM voltage that excites the parasitic capacitances are the main source of CM noise. This CM noise is analysed by calculating the change in CM voltage from one state to another state for single phase shift technique (SPST) measured at LISN terminals. The CM noise for symmetrical and asymmetrical inductor and parasitic capacitors are also analysed using this approach. The analysis is thoroughly verified in LTspice with the parasitics measured from the hardware prototype.
8.	Biocompatible High Entropy Alloys with Excellent Degradation Resistance in a Simulated Physiological Environment J Shittu, M Pole, I Cockerill, M Sadeghilaridjani…H Singh… - ACS Applied Bio Materials, 2020 **Abstract:** Bioimplants are susceptible to simultaneous wear and corrosion degradation in the aggressive physiological environment. High entropy alloys with equimolar proportion of constituent elements represent a unique alloy design strategy for developing bioimplants due to their attractive mechanical properties, superior wear, and corrosion resistance. In this study, the tribo-corrosion behavior of an equiatomic MoNbTaTiZr high entropy alloy consisting of all biocompatible elements was evaluated and compared with 304 stainless steel as a benchmark. The high entropy alloy showed a low wear rate and a friction coefficient as well as quick and stable passivation in simulated body fluid. An increase from room temperature to body temperature showed excellent temperature assisted passivity and nobler surface layer of the high entropy alloy, resulting in four times better wear resistance compared to stainless steel. Stem cells and osteoblast cells displayed proliferation and migratory behavior, indicating in vitro biocompatibility. Several filopodia extensions on the cell periphery indicated early osteogenic

	commitment, and cell adhesion on the high entropy alloy. These results pave the way for utilizing the unique combination of tribo-corrosion resistance, excellent mechanical properties, and biocompatibility of MoNbTaTiZr high entropy alloy to develop bioimplants with improved service life and lower risk of implant induced cytotoxicity in the host body.
9.	Categorization of pedestrian level of service perceptions and accounting its response heterogeneity and latent correlation on travel decisions TM Rahul, M Manoj - Transportation Research Part A: Policy and Practice, 2020 **Abstract:** User perception plays a critical role in pedestrian infrastructure usage. Indeed, the perceptional influence varies across individuals, and it is imperative to consider their response heterogeneity in modelling individual travel intentions. The present study develops a novel framework to understand the pedestrian perception, and further identify their impact on future travel decisions. In this framework, the individual pedestrian perception of an area is captured using a Level of Service (LOS) index, and the overall set of LOS is categorized using a clustering methodology. The future travel behavior is modelled using a single-step estimation that incorporates the effect of both response heterogeneity and latent individual correlation. The proposed framework is utilized in estimating the LOS categorization and the future willingness to walk in the city of Coimbatore, India. The results found a significant response heterogeneity among respondents in Coimbatore, and consequently emphasized the need for incorporating these taste variations in the travel behavior models. An increase in LOS encouraged the respondents to walk, and further, walk longer. Moreover, females were willing to pursue walking and/or walk more distance compared with males. The positive ordinal interval for LOS 'A' to 'C' indicated an acceptability for this LOS range among pedestrians compared with LOS 'E' to 'F' having a negative range. In the individual assessment of LOS variables, almost all study areas were found requiring an improvement with respect to the management of footpath vendors and footpath cleanliness.
10.	Controllable synthesis of tunable aspect ratios novel h-BN nanorods with an enhanced wetting performance for water repellent applications A Kumar, G Malik, K Goyal, N Sardana, R Chandra… - Vacuum, 2020 **Abstract:** One dimensional (1-D) nanostructured layer with tunable aspect ratio holds the prodigious potential for achieving smart surfaces with controlled wettability. Herein, a simple and cost-effective technique was employed to develop the high quality and novel hexagonal boron nitride (h-BN) nanorods. These h-BN nanorods (BNNRs) with tunable aspect ratio contained oriented aligned nanoparticles along the [0001] direction were prepared by wet chemical reaction method using non-toxic precursor (melamine, urea and boric acid). Controlled chemical reactions in applied atmosphere (Ar 90% + NH3 10%) play an important role to transform the morphological growth and tune the aspect ratio (AR) of h-BN nanorods by simply varying the annealing temperature (1100–1300 °C). The correlation between structural, morphological and wetting properties of prepared materials were also investigated in detail. The behavior of wettability was also analyzed in term of water contact angle and surface free energy using two complex models, Wu and Owens & Wendt. Overall, the effect of annealing temperature and atmosphere were accountable to trigger the growth (aspect ratio from ~2.5 to ~5.2) and wetting behavior from hydrophobic to ~ super hydrophobic (contact angle from 127° to 145°.). Produced at 1300 °C, the highly oriented h-BN nanorods with large aspect ratio (AR) ~5.2 and excellent wettability (hydrophobicity ~145°) may be a promising candidate for water

	repellent applications.
11.	Convolution neural network for effective burn region segmentation of color images J Chauhan, P Goyal - Burns, 2020 **Abstract:** Background Burn injuries are one of the most severe forms of wounds and trauma across the globe. Automated burn diagnosis methods are needed to provide timely treatment to the concerned patients. Artificial intelligence is playing a vital role in developing automated tools and techniques for medical problems. However, the use of advanced AI techniques for color images based burn region segmentation is not much explored. Method In this work, we explore the use of deep learning for the challenging problem of burn region segmentation. We prepared a pixel-wise labelled new burn images dataset for segmentation and investigated the efficacy of existing state-of-the-art color images based semantic image segmentation techniques. Lately, we proposed a new convolution neural network (CNN) that uses atrous convolution for encoding rich contextual information and utilizes pre-trained model ResNet-101 for better extraction of low-level and middle-level layer features. Results The proposed approach achieves the state-of-the-art performance on the prepared burn image dataset with 77.6% of Mathews correlation coefficient (MCC) and 93.4% of accuracy. The improvement of 11.6/5.8/6.9/1.2% is observed in precision, Dice similarity coefficient, Jaccard index and specificity, in comparison to the second best performance. Conclusion In this work, we propose a CNN based novel method for performing burn-region segmentation in color images and evaluate it using newly prepared Burn Images dataset. The experimental results illustrate its effectiveness in comparison to existing approaches. Further, the proposed pixel-level segmentation method could be useful in estimating the burn surface area and burn severity in an accurate and time efficient manner.
12.	Delayed Leidenfrost phenomenon during impact of elastic fluid droplets P Dhar, SR Mishra, A Gairola, D Samanta - Proceedings of the Royal Society A, 2020 **Abstract:** This article highlights the role of non-Newtonian (elastic) effects on the droplet impact phenomenon at temperatures considerably higher than the boiling point, especially at or above the Leidenfrost regime. The Leidenfrost point (LFP) was found to decrease with an increase in the impact Weber number (based on the velocity just before the impact) for fixed polymer (polyacrylamide) concentrations. Water droplets fragmented at very low Weber numbers (approx. 22), whereas the polymer droplets resisted fragmentation at much higher Weber numbers (approx. 155). We also varied the polymer concentration and observed that, up to 1000 ppm, the LFP was higher than that for water. This signifies that the effect can be delayed by the use of elastic fluids. We have shown the possible role of elastic effects (manifested by the formation of long lasting filaments) during retraction in the increase of the LFP. However, for 1500 ppm, the LFP was lower than that for water, but had a similar residence time during the initial impact. In addition, we studied the role of the Weber number and viscoelastic effects on the rebound behaviour at 405°C. We observed that the critical Weber number up to the point at which the droplet resisted fragmentation at 405°C increased with the polymer concentration. In

	addition, for a fixed Weber number, the droplet rebound height and the hovering time period increased up to 500 ppm, and then decreased. Similarly, for fixed polymer concentrations like 1000 and 1500 ppm, the rebound height showed an increasing trend up to certain a certain Weber number and then decreased. This non-monotonic behaviour of rebound heights was attributed to the observed diversion of the rebound kinetic energy to rotational energy during the hovering phase. Finally, a relationship between the non-dimensional Leidenfrost temperature and the associated Weber and Weissenberg numbers is developed, and a scaling relation is proposed.
13.	Determination of coefficient of secondary compression in accelerated incremental loading consolidation test M Raheena, RG Robinson - Geotechnical Characterization and Modelling, 2020 **Abstract:** Coefficient of secondary compression is one of the important consolidation properties of fine-grained soils exhibiting high secondary compression. Generally, soils containing significant amount of organic matter exhibit high secondary compression. It is generally determined by performing laboratory one-dimensional incremental loading (IL) consolidation test, in which each increment is allowed for 24 h or more. Typically, conventional one-dimensional IL consolidation test takes about 10–14 days to complete. Therefore, end-of-primary consolidation (EOP) test and rapid one-dimensional consolidation tests were developed in the literature to reduce the duration of conventional IL tests. The limitation of these methods is that coefficient of secondary compression cannot be determined as the specimen is not allowed to reach the secondary compression phase. This paper describes a method of determining coefficient of secondary compression from accelerated incremental load consolidation testing procedure using $t\sqrt{}$ method. In the proposed method, one of the pressure increments is left for sufficiently long time to obtain the linear secondary compression phase in the log t plots. The suggested procedure is validated by comparing the results obtained from the conventional IL consolidation test on four soil samples with varying range of secondary compressibility and plasticity characteristics.
14.	Drive-train selection criteria for n-dof manipulators: basis for modular serial robots library E Singla, S Singh, A Singla - International Journal of Nonlinear Sciences and Numerical Simulation, 2020 **Abstract:** Towards planning a modular library for customized designs of serial manipulators, a trade-off is required between minimum modules inventory and maximum robotic applications to be handled. This paper focusses at the types of modules which are majorly based upon optimized payload capacity of the modular links. To find minimum types of modules in the modular library, an exercise has been performed on a large variety of robotic manipulators, with variations in degrees-of-freedom (dof) between 3 and 9 in number and that in payload capacity between 0 and 5 in kgs. Observing the pattern of the maximum-torque based drive-train selections for all the manipulators in consideration, three types of actuators are selected from a set of Maxon motor-gear assemblies. Subsequently, three types of modules are planned—Heavy (H), Medium (M) and Light (L). Challenge involved is the maximum load estimations for each joint involving variations due to large number of dof, various possible configurations and realistic weight estimation. This paper provides a general recursive framework for optimized drive-train, with one step as determination of maximum load estimation at a joint, and the second step as the selection of appropriate motor-gear assembly for the joint—providing an appropriate weight estimation for critical-configuration evaluation of the next link. The methodology is

	utilized for planning optimized number of modular divisions, for evaluating payload capacity of each division and possible modular combinations for given number of degrees-of-freedom.
15.	Effect of local dissociations in bidirectional transport of driven particles A Jindal, AB Kolomeisky, AK Gupta - Journal of Statistical Mechanics: Theory and Experiment, 2020 **Abstract:** Motivated by the complex processes of cellular transport when different types of biological molecular motors can move in opposite directions along protein filaments while also detaching from them, we developed a theoretical model of the bidirectional motion of driven particles. It utilizes a totally asymmetric simple exclusion process framework to analyze the dynamics of particles moving in opposite directions along the lattice of discrete sites while the particles might also dissociate from the filament in the bulk of the system. Mean-field theoretical arguments supported by extensive Monte Carlo simulations are presented in order to understand how the localized particle dissociations affect the bidirectional dynamics and spontaneous symmetry-breaking phenomena. It is found that changes in the amplitudes and in the symmetry of dissociation rates lead to significant modifications in the dynamic properties and in the stationary phase diagrams. These changes are explained using simple physical arguments. Our theoretical method clarifies some aspects of microscopic mechanisms of complex transport phenomena in biological systems.
16.	Effect of non-Newtonian fluid behavior on forced convection from a cluster of four circular cylinders in a duct, Part I: Power-law fluids M Trivedi, N Nirmalkar, AK Gupta, RP Chhabra - Heat Transfer Engineering, 2020 **Abstract:** Forced convection heat transfer in power-law fluids has been investigated numerically around four identical circular cylinders in a diamond array in a square enclosure. For the laminar flow, the governing equations have been solved numerically over the following ranges of parameters: Reynolds number (5 - 200), Prandtl number (0.7 - 100), power-law index (0.2 - 2) and center-to center gap between cylinders (0.3 - 0.7) to elucidate their influence. The detailed kinematics and engineering parameters are influenced by the gap between the cylinders via the development of multiple secondary flow regions and/or the splitting of incoming fluid stream. The drag on the trailing cylinders with reference to the lead cylinder can be up to ± ∼ 80% higher or lower depending upon the gap between the cylinders, power-law index and Reynolds numbers. In compact arrays, the drag becomes slightly negative due to the reverse flow for certain combinations of power-law index (< 1) and high Reynolds numbers (100 and 200). Similarly, the heat transfer affected by the subsequent cylinders ranges from 50-60% for the second cylinder which drops to ∼10% for the last cylinder. Finally, the functional dependence of the Nusselt number has been consolidated in terms of Reynolds number, Prandtl number, power-law index and the gap ratio.
17.	Effect of non-Newtonian fluid behavior on forced convection from a cluster of four circular cylinders in a duct, Part II: Bingham plastic fluids M Trivedi, N Nirmalkar, AK Gupta, RP Chhabra - Heat Transfer Engineering, 2020 **Abstract:** Extensive results are reported on the flow and heat transfer for Bingham plastic fluids for the same configuration as in Part I over the ranges: Reynolds number (5 − 200), Prandtl number (1−100), and Bingham number (0.01−100) and the gap ratio (0.3 − 0.7). At small Bingham numbers, the results deviate a little from that in Newtonian fluids except for the

	pockets of unyielded material. With the increasing fluid yield stress, the flow field consists of preferred flow channels between the inlet and outlet ports with high shear zones which directly influence the drag and Nusselt number. Depending upon the extent of fluid yielding, the drag on the middle cylinder can be higher by up to ~100% or lower by up to ~90% than that on the upstream cylinder. Similarly, the strong back flow observed at low Bingham numbers and high Reynolds numbers in the rear of the downstream cylinder leads to negative drag. In sparse arrays, the drag of upstream and downstream cylinders is comparable but that on the middle cylinder is always smaller. Similarly, the average heat transfer coefficient for each successive cylinder decreases with respect to the upstream cylinder. For the upper and downstream cylinder, this ratio is about 28-65% depending upon the kinematic conditions. In most cases, the first cylinder offers the maximum heat transfer.
18.	Estimation and Validation of Enhanced Resolution Brightness Temperature Products of SCATSAT-1 S Singh, RK Tiwari, V Sood - IEEE 5th International Conference on Computing Communication and Automation (ICCCA), 2020 **Abstract:** The brightness temperature (Tb) is considered a fundamental climate data record that governs the radiance traveling towards the satellite from the top of the atmosphere. It is used to derive the wind speed, cloud liquid water and sea surface temperature. The optical sensors play a vital role in the retrieval of Tb but also affected by the clouds and different solar illuminations. On the other hand, scatterometer offers the day/night data delivery even in cloudy conditions and insensitive towards solar illuminations. Scatterometer Satellite (SCATSAT-1) based on Ku-band (13.5 GHz), is launched by ISRO (Indian Space Research Organization) on 26 th September 2016. Besides backscattering coefficients (sigma-naught and gamma-naught), SCATSAT-1 also provides the Tb for slices and footprints that are derived from scatterometer noise measurement, expressed in units of the temperature (deg. K). The SCATSAT-1 Level 4 Tb product is available at two different polarization modes i.e. HH and VV. The main objective of this study is to retrieve the Tb at HH and VV over a part of Western Himalayas (Himachal Pradesh, India) using the SCATSAT-1 backscattering and validating the results using MODIS (Moderate Resolution Imaging Spectroradiometer) data. Based on similarity measures, it is found that SCATSAT-1 achieved the well-correlation [R squared 0.8311 (for VV) and 0.8343 (for HH)] with MODIS Tb. This study can be utilized in many remote sensing applications in flood detection or other natural disasters.
19.	Experimental study of miscible viscous fingering with different effective interfacial tension RX Suzuki, FW Quah, T Ban, M Mishra, Y Nagatsu - AIP Advances, 2020 **Abstract:** Viscous fingering (VF) occurs when a more viscous fluid is displaced by a less viscous one in porous media or in Hele-Shaw cells. Generally, VF can be divided into two types: immiscible VF and miscible VF. The typical immiscible finger is wider than the equivalent miscible finger because of interfacial tension. Recently, it has been pointed out that an effective interfacial tension (EIT) is present even in miscible systems when there is a steep concentration gradient of chemical species at the interface. The effects of EIT on miscible VF have so far mainly been studied numerically showing that the fingers become wider owing to EIT. Here, we perform an experimental investigation of the effects of EIT on miscible VF by establishing two solution systems that have different concentration differences but the same viscosity contrast. One is a glycerol solution with a concentration of 99 wt. % and water and has a higher water

	concentration difference of ΔCw = 99 wt. %. The other is a polymer solution with a concentration of 8.5 wt. % and water and has a lower water concentration difference of ΔCw = 8.5 wt. %. We show by direct measurement with a spinning drop tensiometer that the glycerol–water system exhibits greater EIT, and we demonstrate experimentally that typical fingers with high EIT become wider than those with low EIT. We suggest that under the experimental condition employed, the VF in the glycerol–water system with high EIT exhibits a characteristic property of immiscible VF, although it has generally been regarded as a typical representative of classical miscible VF.
20.	Fast Goertzel Algorithm and RLS-Adaptive Filter Based Reference Current Extraction for Grid-Connected System B Singh, CC Reddy - IEEE PES Innovative Smart Grid Technologies Europe (ISGT-Europe), 2020 **Abstract:** In this paper, a smart hybrid Fast Goertzel Algorithm and RLS-Adaptive Filter based control scheme for harmonic elimination, load balancing is presented. The control algorithm is designed for shunt active power filter (SAPF) connected in parallel with grid under distorted load conditions and non-linear load. The function of the fast Goertzel algorithm is to extract the fundamental frequency component with its magnitude and phase from the load currents. This extracted fundamental frequency component is used for estimating the reference currents based on the Recursive Least Squares (RLS) adaptive filter approach. This hybrid FG-RLS (Fast Goertzel-Recursive Least Square) control algorithm retains its behaviour even under load unbalancing and sudden load shutdown. Such improvement helps the adaptive filter for better convergence rate with less computation burden. The performance of the proposed FG-RLS scheme is simulated on three-phase applications to demonstrate its capability for extracting the fundamental component and further estimating reference currents.
21.	Influence of flow pulsations and yield stress on heat transfer from a sphere G Mishra, RP Chhabra - Applied Mathematical Modelling, 2020 **Abstract:** In this work, the momentum and heat transfer characteristics of a time-dependent flow of Bingham plastic fluid over a heated isothermal sphere have been investigated numerically over wide ranges of conditions: Reynolds number, $5 \leq Re \leq 120$, Bingham number, $0.1 \leq Bn \leq 100$, Prandtl number, $0.7 \leq Pr \leq 100$, frequency, $\pi/4 \leq \omega^* \leq \pi$ and amplitude, $0 \leq A \leq 0.8$. The influence of the fluid yield stress and inertia due to the imposed flow pulsations on the flow and thermal fields have been examined in detail. Detailed structure of the flow and temperature fields are analysed in terms of the instantaneous streamlines, isothermal contours, yielded/unyielded zones, surface pressure profiles, time-average drag coefficient and surface- and time-average Nusselt number. The influence of the frequency and amplitude of pulsations on the size of yielded (fluid-like) and unyielded (solid-like) zones is considered in order to understand convective heat transport. The size of yielded zones is seen to be in phase with the imposed pulsating velocity. However, the yield stress effects suppress the influence of flow pulsations. The temporal evolution of the drag coefficient and Nusselt number lag the imposed pulsating flow by different degrees thereby indicating the inherently different evolution of the momentum and thermal boundary layers. Broadly, the pulsating flow conditions may lead to up to 20% augmentation in heat transfer provided there is a moderate degree of advection and/or when the fluid yield stress effects are weak, i.e., small Bingham numbers. Thus, the maximum benefits of pulsating flow accrue in Newtonian fluids only. Finally, the present values of the time-average

	Nusselt number have been consolidated in the form of a predictive expression.
22.	L-histidine controls the hydroxyapatite mineralization with plate-like morphology: Effect of concentration and media N Chauhan, Y Singh - Materials Science and Engineering: C, 2020 **Abstract:** Hydroxyapatite (HA) is the main inorganic component of bone and dentin, and their non-stoichiometric compositions and plate-shaped morphology is responsible for their bioactivity and osteoconductive nature. Collagenous (CPs) and non-collagenous proteins (NCPs) facilitate mineralization and regulate structural properties of HA through their side-chains. The bioactivity of synthetic HA does not usually match with the HA found in bone and, therefore, there is a need to understand the role of biomolecules in bone mineralization in order to develop non-stoichiometric plate-shaped HA for bone grafts. Role of several amino acids has been investigated but the role of L-his has been rarely investigated under physiological conditions even though it is a part of HA inhibitor proteins, like albumin, amelogenin, and histidine-rich proteins. In this study, L-his and L-glu were used to modify the structural properties of HA in different experimental conditions and buffer systems (tris and hepes). The results showed that L-his was able to regulate the plate-shaped morphology of HA in every experimental condition, unlike the L-glu, where the crystal morphology was regulated by experimental conditions. Both amino acids behaved differently in DI water, tris, and hepes buffer, and the media used influenced the precipitation time and structural properties of HA. Hepes and tris buffers also influenced the HA precipitation process. Overall, the studies revealed that L-his may be used as an effective regulator of plate-shaped morphology of HA, instead of large NCPs/proteins, for designing biomaterials for bone regeneration applications and the choice of buffer system is important in designing and evaluating the systems for mineralization. In cell culture studies, mouse osteoblast precursor cells (MC3T3-E1) showed highest proliferation on the bone-like plate-shaped HA, among all the HA samples investigated.
23.	Nanostructuring at elevated temperatures on ion irradiated CoSi binary mixture BK Parida, S Sarkar - AIP Conference Proceedings, 2020 **Abstract:** Nanostructure formation at low energy ion beam sputtering on binary surface varying the substrate temperature has been studied. The surface has been irradiated with Ar+ ion at 700 eV and a fluence of 1.4×1018 ions.cm-2. Co69Si31 surfaces have shown peculiar nanoscale semi-ellipsoidal structures for different surface temperatures (100°-400° C) at an angle incidence of 67°. A periodicity is appeared for comparatively higher temperature perpendicular to ion beam direction. The root mean square (rms) roughness variation has been summarized. Ion beam polishing effect and the thermal diffusion play crucial role in the pattern evolution.
24.	Nitrogen and sulfur co-doped fluorescent carbon dots for the trapping of Hg (ii) ions from water H Kaur, N Kaur, N Singh - Materials Advances, 2020 **Abstract:** An uncomplicated, reliable, and ultrasensitive fluorescent sensor motif based on carbon dots (CDs) co-doped with nitrogen and sulfur atoms has been fabricated using calix[4]arene and benzothiazole moieties for the recognition of toxic mercuric ions (Hg^{2+}) in aqueous medium and the application has been established in Tris–HCl buffer solution, real water samples, and the trapping of Hg^{2+} ions from aqueous medium. It was observed that the fluorescence intensity of the as-synthesized CDs could be entirely quenched in the presence of Hg^{2+} ions due to the electron/energy transfer process between the surface functional groups of

	the CDs and soft closed-shell Hg2+ ions. The proposed nanosensor could proficiently detect Hg2+ ions in aqueous medium with a detection limit of the order of 7.89 nM with high selectivity, sensitivity, and with a relatively low background interference even in a complex medium. The CDs were then further adsorbed on the surface of silica and were investigated for their ability to trap/capture Hg2+ ions using chromogenic and atomic absorption spectroscopy (AAS) method.
25.	Node-weighted centrality: a new way of centrality hybridization A Singh, RR Singh, SRS Iyengar - Computational Social Networks, 2020 **Abstract:** Centrality measures have been proved to be a salient computational science tool for analyzing networks in the last two to three decades aiding many problems in the domain of computer science, economics, physics, and sociology. With increasing complexity and vividness in the network analysis problems, there is a need to modify the existing traditional centrality measures. Weighted centrality measures usually consider weights on the edges and assume the weights on the nodes to be uniform. One of the main reasons for this assumption is the hardness and challenges in mapping the nodes to their corresponding weights. In this paper, we propose a way to overcome this kind of limitation by hybridization of the traditional centrality measures. The hybridization is done by taking one of the centrality measures as a mapping function to generate weights on the nodes and then using the node weights in other centrality measures for better complex ranking.
26.	Numerical simulation of wave propagation across multiple parallel rock joints using DEM R Sebastian, TG Sitharam - Geotechnical Characterization and Modelling, 2020 **Abstract:** The propagation of waves across parallel joints in rock mass involves multiple reflections of waves between joints. Propagation of waves across multiple parallel joints is numerically modeled and presented in this paper using distinct element simulations. The validation of numerical model was performed by comparing wave velocities obtained in laboratory and numerical simulations. For the study on wave propagation across parallel joints, DEM numerical models with varying number of joints were generated. The wave velocities, wave amplitudes and energy flux of waves were monitored. It has been found that as the number of joints in rock mass increases, there is a transition from intermediate wavelength condition to long wavelength condition. The stress waves monitored indicated that there are considerable reflections of waves between joints and waves propagating under intermediate wavelength condition sense the presence of joints. Due to the superposition of waves between joints, the waves may get amplified also.
27.	Optimal floc structure for effective dewatering of polymer treated oil sands tailings D Zhang, T Abraham, T Dang-Vu, J Xu, SP Gumfekar… - Minerals Engineering, 2021 **Abstract:** Synthetic polymeric flocculants such as anionic polyacrylamides are widely used for dewatering mature fine tailings (MFT) generated from oil sands mining operations. Many studies have investigated the effects of polymer properties on dewatering efficiency. However, only a few studies have investigated the reasons for effective dewatering at optimum dosages from the perspective of understanding changes in the internal and external microstructure of the floc. In MFT, clay solids are dispersed in brine (along with trace amounts of bitumen) and are known to have a house-of-card like microstructural arrangement due to electrostatic stabilization. In this study, we investigated why there is maximum dewatering in the specific polyacrylamide (PAM)

	polymer-MFT system at optimum dosage. To understand this, we investigated the morphological changes in the house-of-cards microstructure in terms of porosity and floc density when flocculated at different polymer dosages as well as the corresponding floc strength, size, and re-flocculation tendencies. SEM imaging results showed that at the optimum dosage of 1000 ppm the internal floc microstructure had two different characteristic zones of reduced porosity and open channels, respectively, indicating that this arrangement could have led to an effective squeeze-out of water from the pores. Focused Beam Reflectance Microscopy results indicated that optimum dosage leads to effective dewatering due to flocs formed in the size range of 10–50 μm and 50–150 μm having reduced re-flocculation tendencies. Optimum dosage resulted in the least number of flocs and the reduction of flocs in the size range of 10–50 μm and < 10 μm was maximum while the corresponding increase of flocs in the size range of 50–150 μm was maximum as compared to other dosages. Additionally, the flocs at optimum dosage did not change in number for a given size range of flocs even after 1-hour stirring indicating strong floc formation. These observations are specific for the particular pairing and could form a basis for investigating other polymer-tailing systems.
28.	Orthogonal Signal Generation based PLL using Arbitrary Order Exact Differentiator with Inherent Disturbance Rejection for Single Phase Systems S Muddasani, AVR Teja - The 46th Annual Conference of the IEEE Industrial Electronics Society, 2020 **Abstract:** Use of Derivative based PLL is one of the simplest and fastest solution for phase-locked loops in single phase systems. The dynamics of Derivative-PLL are comparatively better than other methods, but it exhibits high frequency noise amplification and also under performs in non-ideal grid conditions. In this paper, a robust arbitrary order exact differentiator is proposed as a solution to generate noise free, fast and exact orthogonal signal by utilizing second order generalized differentiator method which is used further to formulate a PLL that is immune to high frequency noise and performs well under various disturbances in voltage, frequency, phase, harmonics, noise and DC-offset in grid voltage. The proposed PLL is modeled using MATLAB/SIMULINK and is tested for standard grid conditions. Typical results are reported and are compared with existing PLLs. It is found that the proposed method is not only simple and immune to noise and disturbances but also superior compared to other PLLs.
29.	Progress and Prospective of CZTSSe/CdS interface engineering to combat high open-circuit voltage deficit of kesterite photovoltaics: A critical review K Kaur, M Kumar - Journal of Materials Chemistry A, 2020 **Abstract:** CZTSSe solar cells are considered to be potential and cost-effective alternative solutions to mature photovoltaic technology for meeting future energy demands. However, the current performance of CZTSSe solar cells is limited due to their high voltage deficit. The comparison of figure-of-merits of the two technologies show that CZTSSe has 62% lower open circuit voltage compared to that of 35% for CIGS, with respect to their associated band gaps. Efficient charge separation and extraction at the absorber–buffer (p–n) junction is paramount for mitigating the voltage loss and achieve high photo-conversion efficiency. The rapid progress for achieving high deliverables in CZTSSe is impeded by interface recombination, which is a consequence of poor-quality p–n junction. The inherent association of CZTSSe with secondary phases and defects due to narrow phase stability plays an unfavorable role in producing a good quality interface. The high density of interface defects, unfavorable band alignment, and

	structural inhomogeneities across the interface are some of the leading causes that nurture interface dominant recombination pathways. These interface-related concerns have drawn the scientific community towards interface engineering and modification of the interface to bring closer performance parity between CZTSSe and matured CIGS solar cell technology. Several approaches have attempted to develop favorable interface features that facilitate improved device performance. This work addresses the critical aspects of interface engineering of the absorber–buffer heterojunction in CZTSSe solar cells and the importance of tools that are essential to identify and eradicate the root causes of low efficiency.
30.	Pulse compression favorable thermal wave imaging techniques for non-destructive testing and evaluation of materials R Mulaveesala, V Arora, G Dua - IEEE Sensors Journal, 2020 **Abstract:** This paper highlights the application of pulse compression favorable Frequency Modulated Thermal Wave Imaging (FMTWI) technique for testing and evaluation of Carbon Fibre Reinforced Plastics (CFRP). The concept of InfraRed Image Correlation (IRIC) has been introduced to reconstruct the correlation fringes for the pulse compressed data obtained from the matched filter approach to detect the flat bottom hole defects in a CFRP specimen. Further, comparison has been made with the acquired phasegrams using frequency and time domain based data processing approaches. Obtained results clearly demonstrate the strengths of the proposed IRIC based post-processing scheme in providing the spatio-temporal correlation fringes for thermal Non-Destructive Testing & Evaluation (NDT&E) of CFRP materials.
31.	Self-assembly of imidazolium/benzimidazolium cationic receptors: their environmental and biological applications A Singh, S Sharma, N Kaur, N Singh - New Journal of Chemistry, 2020 **Abstract:** Due to the high affinity of imidazolium and benzimidazolium cations to interact with phosphate and sulfate-based anionic surfactants, micelles of different shapes and properties have been constructed by tailoring the design of organic cations and anionic surfactants. Accumulation of a conjugated aromatic system to such kinds of cationic receptors introduces interesting photophysical properties such as aggregation-induced emission (AIE), and aggregation caused quenching (ACQ), which allows them to be used as a sensor and for catalytic degradation of environmental contaminants. The current review will be focused on the design, synthesis, and characterization of micellar structures with various spectroscopic and electrochemical techniques. The applications of the micellar system to the potential future development of sensors are discussed in the context of recent findings of catalytic and sensing activity of cationic receptors. Additionally, the resemblance of these micelles with lipid bilayer structures (phospholipids), and their interaction with the cell wall of bacteria to eradicate the bacteria, is also discussed.
32.	Solar PV Characteristic Independent Fast Global Maximum Power Point Tracking Algorithm S Singh, AVR Teja - The 46th Annual Conference of the IEEE Industrial Electronics Society, 2020 **Abstract:** This paper proposes a novel maximum power point tracking algorithm for solar PV system that can work even under partial shading conditions. The proposed algorithm is easy to implement, does not depend on any system parameters, and always takes same amount of time for tracking global maximum power point. The algorithm is based on duty ratio variation rather

	than solar PV characteristics for tracking the global maxima. The propositions are simulated using MATLAB/Simulink and typical results are presented. It is shown that tracking time and accuracy can be improved with the variation of switching frequency and the filter inductor (L) and capacitor (C) values used in the boost converter. It is further shown that using the proposed algorithm, global maximum power point with >99% accuracy can be reached within 1 ms.
33.	Surface declination governed asymmetric sessile droplet evaporation P Dhar, RK Dwivedi, AR Harikrishnan - Physics of Fluids, 2020 **Abstract:** This article reports droplet evaporation kinetics on inclined substrates. Comprehensive experimental and theoretical analyses of the droplet evaporation behavior for different substrate declinations, wettability, and temperatures have been presented. Sessile droplets with substrate declination exhibit a distorted shape and evaporate at different rates compared to droplets on the same horizontal substrate, and exhibit more frequent changes in regimes of evaporation. The slip-stick and jump-stick modes are prominent during evaporation. For droplets on inclined substrates, the evaporative flux is also asymmetric and governed by the initial contact angle dissimilarity. Due to a smaller contact angle at the rear contact line, it is the zone of a higher evaporative flux. Particle image velocimetry shows increased internal circulation velocity within the inclined droplets. Asymmetry in the evaporative flux leads to higher temperature gradients, which ultimately enhances the thermal Marangoni circulation near the rear of the droplet where the evaporative flux is highest. A model is adopted to predict the thermal Marangoni advection velocity, and good match is obtained. The declination angle and imposed thermal conditions compete and lead to morphed evaporation kinetics than those of droplets on horizontal heated surfaces. Even weak movements of the contact line alter the evaporation dynamics significantly, by changing the shape of the droplet from an ideally elliptical to an almost spherical cap, which ultimately reduces the evaporative flux. The lifetime of the droplet is modeled by modifying available models for a non-heated substrate, to account for the shape asymmetry. The present observations may find strong implications toward microscale thermo-hydrodynamics.
34.	WikiGaze: Gaze-based Personalized Summarization of Wikipedia Reading Session N Dubey, S Setia, AA Verma, SRS Iyengar - Proceedings of the 3rd Workshop on Human Factors in Hypertext, 2020 **Abstract:** Wikipedia is an open-content encyclopedia that receives billions of page views per month. It has been observed that in a single reading session, Wikipedia users visit multiple articles. To reduce the problems of overload and loss of information, there has been a growing interest in the research community to develop new approaches to present the only necessary information to the users. Automatically generation of personalized summaries is a proven remedy for the information overload problem. In this paper, we propose a technique to generate personalized summaries for Wikipedia articles by analyzing the reading patterns of users. To perform reading pattern analysis, we track eye gaze during the article reading session. Eye gaze analysis helps in identifying the attention distribution of a reader over an article. We extend the proposed approach to generate a summary for multiple articles visited during a user's Wikipedia reading session. We capture a dataset representing the reading pattern of Wikipedia users. We make this dataset publicly available for research community1.